

Models of spherical shells as sources of Majumdar-Papapetrou type spacetimes

Gonzalo García-Reyes*

Departamento de Física, Universidad Tecnológica de Pereira, A. A. 97, Pereira, Colombia

By starting with a seed Newtonian potential-density pair we construct relativistic thick spherical shell models for a Majumdar-Papapetrou type conformastatic spacetime. As simple example, we consider a family of Plummer type relativistic spherical shells. These objects are then used to model a system composite by a dust disk and a halo of matter. We study the equatorial circular motion of test particles around the structures. Also the stability of the orbits is analyzed for radial perturbation using an extension of the Rayleigh criterion. The models considered satisfying all the energy conditions.

arXiv:1608.01918v1 [gr-qc] 5 Aug 2016

* e-mail: ggarcia@utp.edu.co

I. INTRODUCTION

Relativistic spherical shells are important in two contexts, in astrophysics as models of elliptical galaxies, bulges of disc galaxies and dark matter haloes, and general relativity as sources of vacuum gravitational fields, cosmological models, gravitational collapse, among others [1, 2]. The pioneering work on relativistic shells is due to Israel [3], who also specialized his general framework to spherical symmetry [4]. Relativistic spherical shells with varying thickness were studied in [5, 6] for a Schwarzschild type conformastatic spacetime. Thin shells representing the field of a disk are also important to model galaxies, accretion disks, and the superposition of a black hole and a galaxy. Static thin disks without radial pressure were first studied by Bonnor and Sackfield [7], and Morgan and Morgan [8], and with radial pressure also by Morgan and Morgan [9]. Several classes of exact solutions of the Einstein field equations corresponding to static thin disks with or without radial pressure have been obtained by different authors [10–16]. Rotating thin disks that can be considered as a source of a Kerr metric were presented by Bičák and Ledvinka [17], while rotating disks with heat flow were studied by González and Letelier [18]. The exact superposition of a disk and a static black hole was first considered by Lemos and Letelier in Refs. [19, 20]. Disk-like matter distribution surrounded by a material halo have been studied in [21–24].

In this work, we consider models of spherical thick shells for a Majumdar-Papapetrou type conformastatic spacetime. The models are constructed from a seed Newtonian potential-density pair. The formalism used allows to build different spherically symmetric sources for this spacetime such as spheres, spherical shells, disks and haloes. As a simple application, we construct a family of Plummer type relativistic spherical shells. These objects are then used to construct dust disk models surrounded of haloes of matter. The structures considered are essentially of infinite extension. However, since the energy density decreases rapidly one can define a cut off radius and, in principle, to consider these objects as finite.

The paper is organized as follows. In Sect. II we present the method to construct different spherical configurations of matter from a Newtonian potential-density pair in the particular case of a Majumdar-Papapetrou type conformastatic spacetime. In Sect. III the formalism is employed to build a family of Plummer type relativistic spherical shell, and then in Sect. IV we model from them a system composite by a dust disk and a halo of matter. In each case we study the equatorial circular motion of test particles around the structures. Also the stability of the orbits is analyzed for radial perturbation using an extension of the Rayleigh criterion [25, 26]. Finally, in Sect. V we summarize and discuss the results obtained.

II. MAJUMDAR-PAPAPETROU TYPE FIELDS AND SPHERICAL STRUCTURES

We consider a conformastatic spacetime [27, 28] in spherical coordinates (t, r, θ, φ) and in the particular form

$$ds^2 = -e^{2\psi} dt^2 + e^{-2\psi} (dr^2 + r^2 d\theta^2 + r^2 \sin^2 \theta d\varphi^2), \quad (1)$$

where $\psi(r)$. These fields can be called Majumdar-Papapetrou type fields due to its known use in context of electrostatic fields [29, 30]. The Einstein field equations $G_{ab} = 8\pi G T_{ab}$ yield the following non-zero components of the energy-momentum tensor

$$T^t{}_t = -\frac{1}{8\pi G} e^{2\psi} (2\nabla^2 \psi - \nabla \psi \cdot \nabla \psi), \quad (2a)$$

$$T^\theta{}_\theta = T^\varphi{}_\varphi = \frac{1}{8\pi G} e^{2\psi} \nabla \psi \cdot \nabla \psi, \quad (2b)$$

$$T^r{}_r = -\frac{1}{8\pi G} e^{2\psi} \nabla \psi \cdot \nabla \psi. \quad (2c)$$

In terms of the orthonormal tetrad $e_{(a)}{}^b = \{V^b, X^b, Y^b, Z^b\}$, where

$$V^a = e^{-\psi} \delta_t^a, \quad X^a = e^\psi \delta_r^a, \quad (3a)$$

$$Y^a = \frac{e^\psi}{r} \delta_\theta^a, \quad Z^a = \frac{e^\psi}{r \sin \theta} \delta_\varphi^a, \quad (3b)$$

the energy-momentum tensor can be written as

$$T^{ab} = \rho V^a V^b + p_r X^a X^b + p_\theta (Y^a Y^b + Z^a Z^b), \quad (4)$$

so that the energy density is given by $\rho = -T^t{}_t$, and the stresses (pressure or tensions) by $p_i = T^i{}_i$. In order to have a physically meaningful matter distribution the components of the energy-momentum tensor must satisfy the

energy conditions. The weak energy condition requires that $\rho \geq 0$, whereas the dominant energy condition states that $|\epsilon| \geq |p_i|$. The strong energy condition imposes the condition $\rho_{eff} = \rho + p_r + p_\theta + p_\varphi \geq 0$, where ρ_{eff} is the “effective Newtonian density”. For the matter tensor (2a)-(2c) these conditions are equivalent to [24]

$$\nabla^2 \psi \geq \nabla \psi \cdot \nabla \psi, \quad (5)$$

which can be written as

$$\nabla^2 \Phi \geq 0, \quad (6)$$

with

$$\Phi = -e^{-\psi} + 1. \quad (7)$$

The inequality (6) can be satisfied by requiring that Φ satisfies the Poisson equation

$$\nabla^2 \Phi = 4\pi G \rho_N, \quad (8)$$

or the equation of Laplace. In this case there is only a family of asymptotically flat solutions, $\Phi = -c/r$, being c a constant.

Using (7) and (8), the physical quantities associated with the matter distribution take the form

$$\rho = \frac{1}{8\pi G(1-\Phi)^3} \left(8\pi G \rho_N + \frac{\Phi_{,r}^2}{1-\Phi} \right), \quad (9a)$$

$$p_\theta = p_\varphi = \frac{1}{8\pi G} \frac{\Phi_{,r}^2}{(1-\Phi)^4}, \quad (9b)$$

$$p_r = -\frac{1}{8\pi G} \frac{\Phi_{,r}^2}{(1-\Phi)^4}, \quad (9c)$$

and for the average pressure we have

$$p = \frac{1}{3}(p_r + p_\theta + p_\varphi) = \frac{1}{24\pi G} \frac{\Phi_{,r}^2}{(1-\Phi)^4}. \quad (10)$$

Thus, given a seed Newtonian potential-density pair (Φ, ρ_N) we can construct for conformastatic fields different models of spherical compact objects such as spheres, spherical shells, disks and haloes.

A. Motion of particles and stability

We will now analyze the motion of test particles around the structures on the plane $\theta = \pi/2$. For equatorial circular orbits the 4-velocity u^a of the particles with respect to the coordinates frame has components $u^a = u^t(1, 0, 0, \omega)$ where $\omega = u^\varphi/u^t = \frac{d\varphi}{dt}$ is the angular speed of the test particles. For the spacetime (1), the equation for the geodesic motion of the particle is given by

$$g_{ab,r} u^a u^b = 0, \quad (11)$$

from which we get

$$\omega^2 = -\frac{g_{tt,r}}{g_{\varphi\varphi,r}}. \quad (12)$$

On the other hand, u^t obtains normalizing u^a , that is requiring $g_{ab} u^a u^b = -1$, so that

$$(u^t)^2 = -\frac{1}{g_{\varphi\varphi}\omega^2 + g_{tt}}. \quad (13)$$

With respect to the orthonormal tetrad (3a)-(3b) the 3-velocity has components

$$v^{(i)} = \frac{e^{(i)}_a u^a}{e^{(0)}_b u^b}. \quad (14)$$

For equatorial circular orbits the only nonvanishing velocity component is given by

$$(v^{(\varphi)})^2 = v_c^2 = -\frac{g_{\varphi\varphi}}{g_{tt}}\omega^2, \quad (15)$$

which represents the circular speed (rotation profile) of the particle as seen by an observer at infinity. Thus we obtain

$$v_c^2 = \frac{r\psi_{,r}}{1 - r\psi_{,r}}. \quad (16)$$

Another quantity related with the geodesic motion of the particles is the specific angular momentum of a particle rotating at a radius r , defined as $h = g_{\varphi\varphi}u^\varphi$. For the plane $\theta = \pi/2$, we have

$$h^2 = \frac{r^2 e^{-2\psi} v_c^2}{1 - v_c^2}. \quad (17)$$

This quantity can be used to analyze the stability of the particles against radial perturbations. The condition of stability,

$$\frac{d(h^2)}{dr} > 0, \quad (18)$$

is an extension of the Rayleigh criteria of stability of a fluid in rest in a gravitational field [26].

For the above spherical distribution these quantities give

$$v_c^2 = \frac{v_{Nc}^2}{1 - \Phi - v_{Nc}^2}, \quad (19a)$$

$$h^2 = \frac{r^2(1 - \Phi)^2 v_{Nc}^2}{1 - \Phi - 2v_{Nc}^2}, \quad (19b)$$

where $v_{Nc}^2 = r\Phi_{,r}$ is the Newtonian circular speed.

III. PLUMMER TYPE SPHERICAL SHELL MODELS

A simple Newtonian potential-density pair that satisfies the condition (6) is [5]

$$\Phi = -\frac{GM}{(r^n + b^n)^{1/n}}, \quad (20a)$$

$$\rho_N = \frac{M(n+1)b^n r^{n-2}}{4\pi(r^n + b^n)^{2+1/n}}, \quad (20b)$$

where b is a non-zero constant with the dimension of length and $n \geq 2$. For $n = 2$ the potential-density pair (20a) and (20b) reduces to Plummer's spherical model [31, 32] for globular clusters which has a mass distribution concentrated at center and for $n \geq 3$ describes a shell-like matter distribution. The Newtonian circular speed is given by

$$v_{Nc}^2 = \frac{GM r^n}{(r^n + b^n)^{1+1/n}}. \quad (21)$$

In this case the metric function ψ is given by

$$\psi = -\ln \left[1 + (GM/b) (\tilde{r}^n + 1)^{-1/n} \right], \quad (22)$$

where $\tilde{r} = r/b$. The relativistic expressions for the energy density and average pressure are

$$\rho = \frac{M\tilde{r}^{n-2} \left[2(n+1)[(\tilde{r}^n + 1)^{1/n} + GM/b] + (GM/b)\tilde{r}^n \right]}{8\pi b^3 (\tilde{r}^n + 1)^{2-2/n} \left[(\tilde{r}^n + 1)^{1/n} + GM/b \right]^4}, \quad (23a)$$

$$p = \frac{GM^2 \tilde{r}^{2n-2}}{24\pi b^4 (\tilde{r}^n + 1)^{2-2/n} \left[(\tilde{r}^n + 1)^{1/n} + GM/b \right]^4}. \quad (23b)$$

The tangential speed and angular momentum obtain directly replacing (20a) and (21) in equations (19a) and (19b).

In Figures 1 (a) - (b) we show the energy density $\tilde{\rho} = \frac{b^3}{M}\rho$ and the average pressure $\tilde{p} = \frac{b^4}{GM^2}p$ for the relativistic shell with $n = 3, n = 6, n = 9$, and $b = MG$, as functions of \tilde{r} . We see that these quantities vanish on $\tilde{r} = 0$ which suggests a shell-like matter distribution, reach a maximum and then decrease rapidly with \tilde{r} . This permits to define a cut off radius r_c and, in principle, to model these structures as a compact object. These quantities become more concentrated when n is increased. We also observe that the energy is everywhere positive in accordance with the weak energy condition.

In Figures 1 (c) - (d) we plot, as functions of \tilde{r} , the curves of tangential speed (rotation curves) v_c and the specific angular momentum $\tilde{h} = h/b^2$ for the same value of the parameters. We see that the particles speed always is less than light speed. We also observe that the increasing n makes more relativistic the motion of particles and unstable the orbits against radial perturbation.

IV. DUST DISKS SURROUNDED BY HALOES

Exact solutions of the Einstein field equations which represent the field of a disk can be obtained by writing the metric (1) in cylindrical coordinates (t, R, z, φ)

$$ds^2 = -e^{2\psi(R,z)}dt^2 + e^{-2\psi(R,z)}(dR^2 + dz^2 + R^2d\varphi^2), \quad (24)$$

and using the well known “displace, cut and reflect” method that was first used by Kuzmin [33] and Toomre [34] to constructed Newtonian models of disks, and later extended to general relativity [14, 15, 17, 18]. Given a solution of the Einstein-Maxwell equation, this procedure is mathematically equivalent to apply the transformation $z \rightarrow |z| + a$, with a constant. The method is the gravitational version of the method of images of electrostatic.

The content of matter on the disks can be analyzed using the formalism of distributions in curved spacetimes [3, 4, 35–37]. For the metric (24) obtains a dust (zero pressure) disk with surface energy density [38]

$$\epsilon = \frac{1}{2\pi G} e^{\psi} \psi_{,z}. \quad (25)$$

In addition, the tangential speed v_c and the specific angular momentum h for geodesic motion of test particles on the disks plane are given by

$$v_c^2 = \frac{R\psi_{,R}}{1 - R\psi_{,R}}, \quad (26a)$$

$$h^2 = \frac{R^2 e^{-2\psi} v_c^2}{1 - v_c^2}. \quad (26b)$$

All the quantities are evaluated at $z = 0^+$.

Now when this procedure is applied to the above structures with $0 \leq a \leq r_c$, one obtains at points with $z > 0$ a matter spherical cap corresponding to a sphere with center located at point $(R, z) = (0, -b)$, and when $z < 0$ a matter cap of a sphere with center at $(R, z) = (0, b)$. The discontinuity in the normal derivative of the metric tensor through the plane $z = 0$ introduces a planar matter distribution which is interpreted as the field of a thin disk. The result in this case is a system composite by dust disks surrounded by a halo of matter (figure 2).

For the potential-density pair (20a) and (20b) we have

$$\psi = -\ln \left[1 + \frac{GM}{b} \left([\tilde{R}^2 + (|\tilde{z}| + \tilde{a})^2]^{n/2} + 1 \right)^{-1/n} \right], \quad (27)$$

where $\tilde{R} = R/b$, $\tilde{a} = a/b$ and $\tilde{z} = z/b$, and the surface density energy is

$$\epsilon = \frac{GM\tilde{a}\tilde{r}^{n-2}}{2\pi(\tilde{r}^n + 1)[1 + (GM/b)(\tilde{r}^n + 1)^{1/n}][MG/b + (\tilde{r}^n + 1)^{1/n}]}, \quad (28)$$

where $\tilde{r} = \sqrt{\tilde{R}^2 + \tilde{a}^2}$.

In Fig. 3 we plot the surface energy density ϵ , the tangential speed v_c and the specific angular momentum for disks with $n = 3, n = 6, n = 9$, and $\tilde{a} = b = MG = 1$, as functions of \tilde{R} . We see that the energy is everywhere positive, its maximum occurs in the center of the disk, and it vanishes sufficiently fast as r increases. When the parameter n is increased, the energy density increases. We observe that circular speed of particles is always a quantity less than the speed of light and that the increasing of n makes more relativistic the orbits. In all cases the motion of particles is stable against radial perturbation. The same behavior is observed for other values of parameter.

V. DISCUSSION

Spherical shell models for a Majumdar-Papapetrou type conformastatic spacetime were studied, using as seed a Newtonian potential-density pair. The formalism presented allows to construct different relativistic spherical configurations of matter such as spheres, spherical shells, disks and haloes. The method was illustrated in the case of a family of Plummer type relativistic thick spherical shells. These objects were then used to construct models of dust disks surrounded by a halo of matter. The structures considered satisfied all the energy conditions.

REFERENCES

-
- [1] J. Kijowski , G. Magli and D. Malafarina, *Gen. Relativ. Gravit.* **38**, 1697 (2006).
 - [2] J. Kijowski , G. Magli and D. Malafarina, *Int. J. Mod. Phys. D* **18**, No. 12, 1801 (2009).
 - [3] E. Israel, *Nuovo Cimento* **44B**, 1 (1966).
 - [4] E. Israel, *Nuovo Cimento* **48B**, 463 (1967).
 - [5] D. Vogt and P. S. Letelier, *Mon. Not. Roy. Astron. Soc.* **402**, 1313 (2010).
 - [6] D. Vogt and P. S. Letelier, *Mon. Not. Roy. Astron. Soc.* **406**, 2689 (2010).
 - [7] W. A. Bonnor and A. Sackfield, *Commun. Math. Phys.* **8**, 338 (1968).
 - [8] T. Morgan and L. Morgan, *Phys. Rev.* **183**, 1097 (1969).
 - [9] L. Morgan and T. Morgan, *Phys. Rev. D* **2**, 2756 (1970).
 - [10] D. Lynden-Bell and S. Pineault, *Mon. Not. R. Astron. Soc.* **185**, 679 (1978).
 - [11] A. Chamorro, R. Gregory, and J. M. Stewart, *Proc. R. Soc. London* **A413**, 251 (1987).
 - [12] P.S. Letelier and S. R. Oliveira, *J. Math. Phys.* **28**, 165 (1987).
 - [13] J. P. S. Lemos, *Class. Quantum Grav.* **6**, 1219 (1989).
 - [14] J. Bičák, D. Lynden-Bell, and J. Katz, *Phys. Rev. D* **47**, 4334 (1993).
 - [15] J. Bičák, D. Lynden-Bell, and C. Pichon, *Mon. Not. R. Astron. Soc.* **265**, 126 (1993).
 - [16] G. A. González and O. A. Espitia, *Phys. Rev. D* **68**, 104028 (2003).
 - [17] J. Bičák and T. Ledvinka, *Phys. Rev. Lett.* **71**, 1669 (1993).
 - [18] G. A. González and P. S. Letelier, *Phys. Rev. D* **62**, 064025 (2000).
 - [19] J. P. S. Lemos and P. S. Letelier, *Class. Quantum Grav.* **10**, L75 (1993).
 - [20] J. P. S. Lemos and P. S. Letelier, *Phys. Rev. D* **49**, 5135 (1994).
 - [21] D. Vogt and P. S. Letelier, *Phys. Rev. D* **68**, 084010 (2003).
 - [22] A. C. Gutiérrez-Piñeres, G. A. González, and H. Quevedo, *Phys. Rev. D* **87**, 044010 (2013).
 - [23] A. C. Gutiérrez-Piñeres, *Gen. Relativ. Gravit.* **47**, No. 5, 54 (2015).
 - [24] G. A. González and O. M. Pimentel, *Phys. Rev. D* **93**, 044034 (2016).
 - [25] Lord Rayleigh, 1917, *Proc. R. Soc. London A*, **93**, 148
 - [26] L. D. Landau and E. M. Lifshitz, *Fluid Mechanics*(Addison-Wesley, Reading, MA, 1989).
 - [27] J. L. Synge, *Relativity: The General Theory* (North- Holland, Amsterdam, 1966).
 - [28] H. Stephani, D. Kramer, M. McCallum, C. Hoenselaers, and E. Herlt, *Exact Solutions of Einsteinss Field Equations* (Cambridge University Press, Cambridge, England, 2003).
 - [29] S. D. Majumdar, *Phys. Rev.* **72**, 390 (1947).
 - [30] A. Papapetrou , *Proc. Roy. Soc. (London)* **A51**, 191 (1947).
 - [31] H. C. Plummer, *MNRAS* **71**, 460 (1911).
 - [32] J. Binney J and S. Tremaine S, 2008, *Galactic Dynamics*, 2nd edn. Princeton Univ. Press, Princeton, NJ.
 - [33] G. G. Kuzmin 1956, *Astron. Zh.*, **33**, 27 (1956).
 - [34] A. Toomre, *Ap. J.*, **138**, 385 (1962).
 - [35] A. Papapetrou and A. Hamouni, *Ann. Inst. Henri Poincaré* **9**, 179 (1968)
 - [36] A. Lichnerowicz, *C.R. Acad. Sci.* **273**, 528 (1971)
 - [37] A. H. Taub, *J. Math. Phys.* **21**, 1423 (1980)
 - [38] G. García-Reyes and O. A. Espitia, *Gen. Relativ. Gravit.* **46**, 1674 (2014).

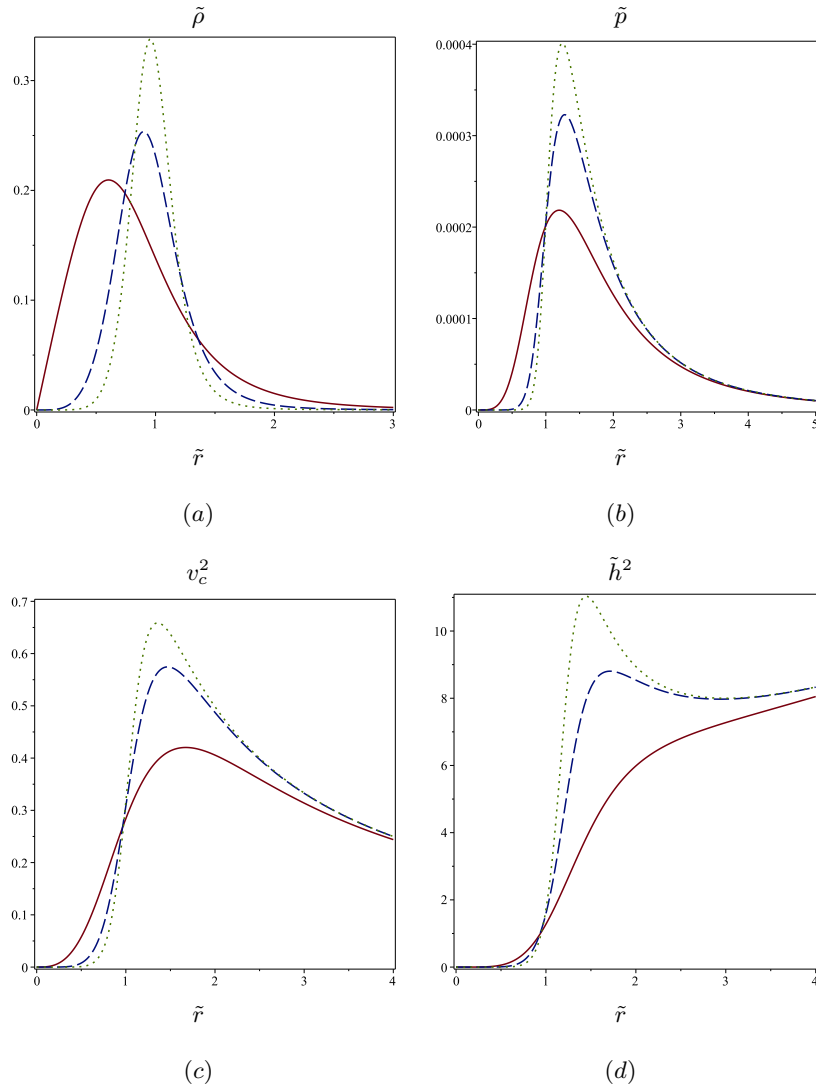


FIG. 1. (a) The energy density $\tilde{\rho}$, (b) the average pressure \tilde{p} , (c) the circular speed v_c , and (d) the specific angular momentum \tilde{h} for the relativistic shells with $n = 3$ (solid curves), $n = 6$ (dashed curves), $n = 9$ (dotted curves), and $b = MG$, as functions of \tilde{r} .

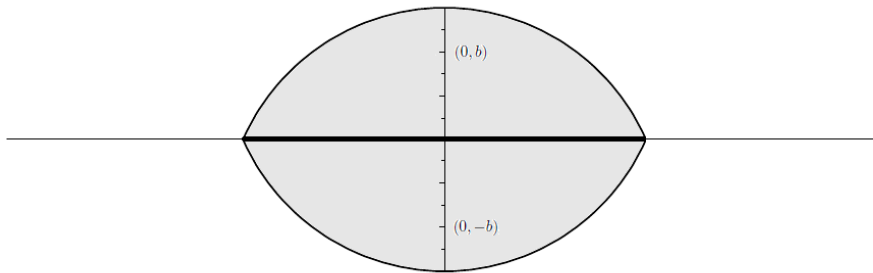


FIG. 2. Schematic representation of the system disk plus halo using the “displace, cut and reflect” method. The points $(0, -b)$ and $(0, b)$ are the centers of spheres corresponding to the spherical caps located above and below of the disk, respectively.

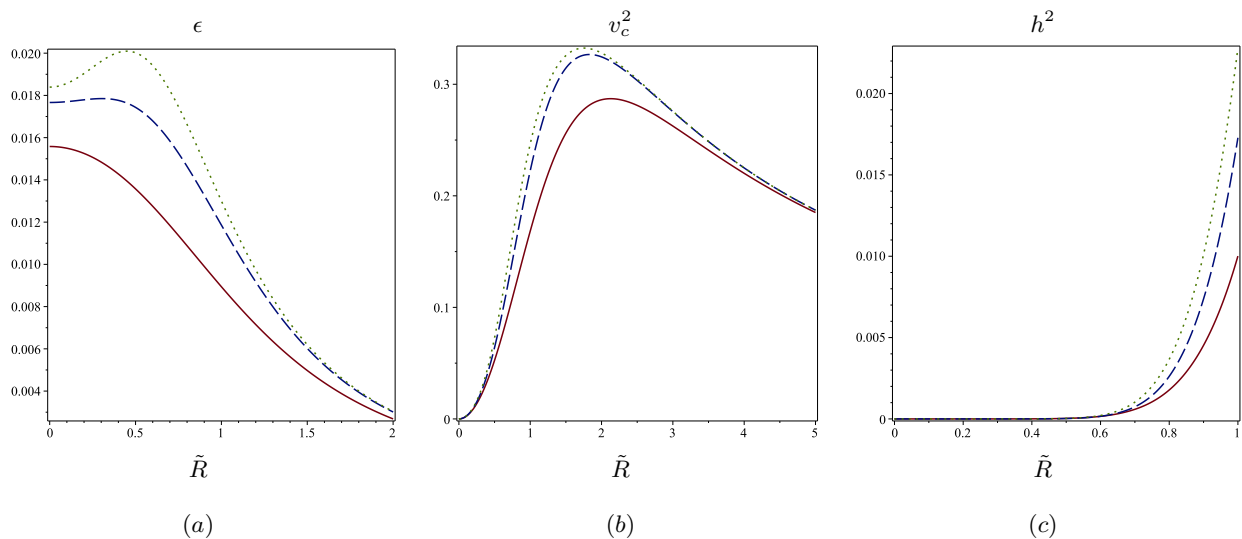


FIG. 3. (a) The surface energy density $\tilde{\epsilon}$, (b) the tangential speed (rotation curves) v_c and (c) the specific angular momentum h for the relativistic disk with $n = 3$ (solid curves), $n = 6$ (dashed curves), $n = 9$ (dotted curves), and $\tilde{a} = b = MG = 1$, as functions of \tilde{R}